Geotechnical Engineering in the XXI Century: Lessons learned and future challenges
N.P. López-Acosta et al. (Eds.)

doi:10.3233/STAL190078

Granular Mechanics of the Shear Strength of Normally Consolidated Clays

Calixtro YANQUI[1]
San Agustin National University of Arequipa, Peru

Abstract. Experiments have shown that the angle of friction obtained in the consolidated-drained test of normally consolidated clays is related, in some way, to the plasticity index or the liquid limit. In this paper, it is demonstrated that this relation shows up because of the discrete nature of clays, whose properties become clear when they are modeled as a packing of spheres. When the diagram of contacts is mapped into the Casagrande's diagram of compression, four intervals show up: one for a dense packing, one for a loose packing, and two impossible; with two points for the critical state. In general, a packing has the same void ratio for two different angles of contact, one dilatant and another contractive. As a normally consolidated clay sample is contractive, it is demonstrated that the angle of friction is independent of the initial water content. But, for a clay geological formation, the friction angle varies according to the features of each layer, following the equation of dense critical state, which fits very well with the experimental data.

Keywords. Clay shear strength, granular packings, clay structure.

1. Introduction

It is a well-established fact that the strength behavior of fine-grained soils is similar to that of sands. Like loose sands, normally consolidated and lightly overconsolidated clays show a gradual increase in shear stress as the shear strain increases until the critical state shear strength is attained, and the volume compresses until a critical state void ratio is reached. Like dense sands, heavily overconsolidated clays show a rapid increase of shear stress up to a peak value and then decrease to reach the critical state shear strength, and the volume expands until a critical state void ratio is reached [1]. Because of this similarities, it is concluded that the theory of packings, using to study sands, is applicable to clays, mainly for a normally consolidated clays. To do that, the real clay structure must be known.

By using the scanning electron microscopy, the fabric of clay soils has become clear. According to Yong and Sheeran [2], clay soils are an assemblage of aggregates called peds. A ped in turn is an assemblage of small aggregates called clusters. A cluster is an assemblage of submicroscopic aggregates called domains. A domain is an assemblage of clay particles. Other authors classify the clay soil structure into two classes: elementary particle arrangements, and particle assemblages. The first includes clay, silt or sand interactions; and the second refers to units with definable physical boundaries and specific functions, consisting of elementary particle arrangements,

[1] Cooperativa Universitaria B – 11, Arequipa, Perú. E-mail: cyanqui@unsa.edu.pe

clothed or linked by connectors [3]. In the present work, it is established that, whatever the complexity of its structure, clays can be represented as packings of ordered spheres.

2. Characteristics of packings of spheres

The voids content of any soil is the simplest manifestation of its granular structure. Among other quantities, the void ratio, e, and the specific volume or voluminosity, $\upsilon=1+e$, are the most useful. In particular, whatever the packing type, it is always possible to choose a parallelepiped as a primitive cell whose vertices are the centers of eight neighboring spheres, not necessarily all in contact (Figure 1a). The volume of the parallelepiped is a known quantity, and the sum of the eight spherical triangles defined by the faces of this element is equal to the volume of the solid sphere of diameter D. Therefore, the voluminosity of a packing of spheres, υ_ϕ, in given by:

$$\upsilon_\phi = \frac{6abc}{\pi D^3}\sin\alpha\cos\varsigma \tag{1}$$

where a, b, and c are the lengths of the edges of the parallelepiped, α, the acute angle formed by the two edges of the horizontal face, and ς, the azimuthal angle of the non-horizontal edge (Figure 1b).

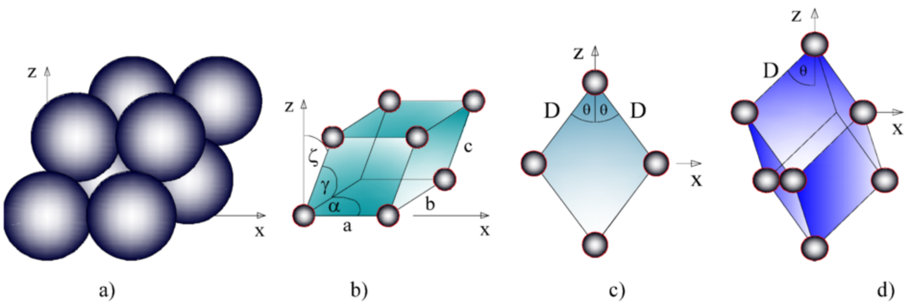

Figure 1. a) Basic packings of spheres, b) General polyhedral representation of a packing of spheres, c) Rhombic or two-dimensional compression model, d) Axial rhombohedron or three-dimensional compression model.

The mechanical behavior of granular materials can be modeled by properly orienting the packing, regarding that strain is due to the movement of the spheres with respect to their neighbors at points of contact. The rhombohedron is one of the crystallographic cell that meets this requirement. The twelve edges of this polyhedron are of the same length, and equal to the diameter of the sphere D (Figure 1a). The shear strain is appropriately described by a horizontal-face rhombohedron, in which $a=b=c=D$, and $\zeta=\beta$ (Figure 1b); the two-dimensional axial compression, by a rhombus, in which $a=b=c=D$, and $\zeta=\theta$ (Figure 1c), and the three-dimensional compression, by a rhombohedron with the major diagonal being vertical (Figure1d), where $\alpha=60°$, $a=b=D\sqrt{3}\sin\theta$, $c=D$ and $\zeta=\theta$. The contact lines are defined by β and θ.

Although it is valid for any kind of packing, Eq. (1) is plotted in (x, e) plane for the contact circumference of a rhombic cell (Figure 2a). In this diagram, the dual character of the packings becomes evident, since for two values of the angle of the line of contact there is a single value of the void ratio (Figure 2b). An interpretation considers the two angles of the contact line describing the active state only. In this case, the analysis of Eq. (1), as a path, shows that the graph has two branches: one ascending and other descending, reaching a maximum value, related to the loosest state of the packing, when $\beta=0°$, for the prismatic cell; $\theta=45°$, for the rhombic cell (Figure 2b), and $\theta=\arccos(1/\sqrt{3})=54.74°$, for the axial rhombohedric cell. In terms of the volume change, the first branch describes a dilatant packing and the second, a contractive packing.

When the critical state in the (e, σ) plane, called compression diagram (Figure 2d), obtained from the stress-strain of the two extreme states of sand (Figure 2c), is mapped into the (x, e) diagram (Figure 2b), the meaning of the critical state result evident: it is different from the loosest state, as assumed by some authors, and is defined by two points. A mapping of the respective paths, reveals that the path of the void ratio is divided into four sections: one dilatant, one contractive and two impossible. The critical state of packings is given by the following law: $e_{dilatant} = e_{contractive}$.

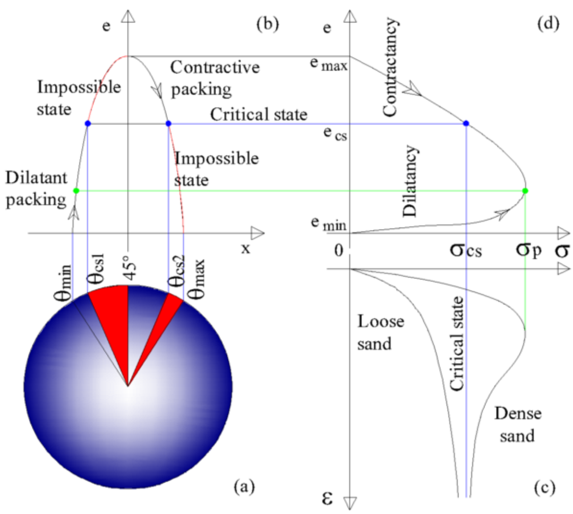

Figure 2. Mapping of packing and compression parameters: a) Circumference of contact between spheres. b) e-θ or e-x plane, showing the duality of the rhombic packing. c) Stress-strain curves for dense and loose sands in the triaxial compression test. d) Casagrande's diagram of compression [4].

3. Contact forces in packings

In a dilatant packing, stresses are transmitted as chains of forces [5, 6]. For instance, in a dilatant rhombic packing of horizontal diagonal S, the forces of contact that concur to a sphere in the one-dimensional compression test have the magnitude: $F=P/[2\cos\theta]$ or $F=Q/[2\sin\theta]$, where P and Q are vertical and horizontal forces, respectively; which are related to the principal stresses by $P=\sigma_1 S$ and $Q=\sigma_3 S\tan\theta$. Eliminating F, the relationship: $\sigma_3=\sigma_1 \tan^2\theta$ is obtained [5]. Likewise, for a rhombohedric packing, $2\sigma_3=\sigma_1\tan^2\theta$ is found. In both cases, the force F is one link of the chain of contact forces. Since $\sigma_3=\sigma_1 K_0$, the relationships $K_0=\tan^2\theta$ and $K_0=\tan^2\theta/2$ are obtained, respectively. From the limit equilibrium of an infinite slope of dense granular soil, the relationships $\cot^2\theta=1+2\tan^2\varphi$ and $2\cot^2\theta=1+3\tan^2\varphi$, are attained, respectively [7], where φ is the peak friction angle. Eliminating the angle θ yields the following equations, for the rhombic and the rhombohedric packings, respectively:

$$K_0=\frac{1}{1+2\tan^2\varphi} \quad ; \quad K_0=\frac{1}{1+3\tan^2\varphi} \tag{2}$$

Figure 3 compares Eq. (2) with the experimental friction angle of the consolidated drained test on several normally consolidated and slightly overconsolidated clay soils, showing a good correspondence.

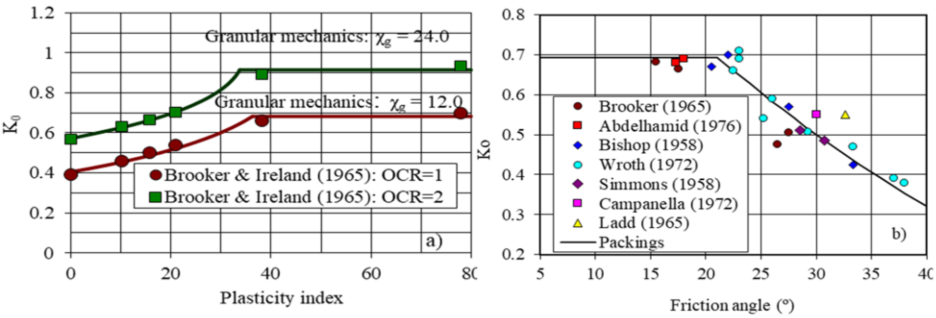

Figure 3. The coefficient of lateral pressure at rest as a function of a) the plasticity index, for a clay [8], and b) the consolidated drained friction angle, for several clays (Compiled by Holtz and Kovacs [9]).

In a contractive packing, the forces of contact acting on a sphere are given by $F=P/[2\cos(\theta-\delta)]$ or $F=Q/[2\sin(\theta-\delta)$, where δ is the angle of obliquity. Since the transmission of the forces occurs by the slip of a sphere over another, the plane on which acts the force F is perpendicular to the contact line; so that: $P=\sigma_1 S$ and $Q=\sigma_3 S\tan\theta$. Then, $\sigma_3=\sigma_1\cot\theta\ \tan(\theta-\delta)$. This expression is similar to the equation obtained by Rowe [10]. It follows that, for a packing to be in contractive state, the following condition must be fulfilled: $\theta \geq 45°$; and, for the same packing to be in active state, the condition $\delta > 0°$ must be fulfilled. Under these conditions, the failure state is reached when the stress ratio is a minimum. Besides, the ultimate angle of obliquity is the friction angle at the critical state; that is, $\delta = \varphi_{cs}$, and $\sigma_3=\sigma_1 \tan^2(45°- \varphi_{cs}/2)$.

4. The packing of fine grained soils

The fine-grained soil fabric, proposed by Yong and Sheeran [2], idealized in figure 4a, may be described in terms of the voluminosity of the packing of each unit as follows: $\upsilon=V/V_{pe}$, $\upsilon_1=V_{pe}/V_{cl}$, $\upsilon_2=V_{cl}/V_{do}$, $\upsilon_3=V_{do}/V_s$, where V, V_{pe}, V_{cl}, V_{do}, and V_s, stand for the volumes of the total sample, the ped, the cluster, the domain, and the clay particle, respectively. The progressive substitution of these quantities yields the fundamental law of clays: $\upsilon=\upsilon_1\upsilon_2\upsilon_3$.

The fabric proposed by Collins and McGown [3] may be represented by a unique flocculated packing, arranged through connectors along the edge of a cell, as shown in Figure 4b. The sphere submerged in water is described by the ratio: $\chi_v= (D_v/D)^3$ =

$(1+2a_v/D)^3$, where a_v is the thickness of the double layer (Figure 4c). The sphere of contact, that entails the shape and angularity of a particle, may be described by the ratio: $\chi_a = (D_c/D_v)^3$, where D_c is the diameter of contact between two neighboring particles (Figure 4c). The total volume for a packing of equal size spheres is given by: $V = (1+N)^3 abc \sin\alpha \cos\zeta$, where N is the number of particles at the edge, except those of the corner of the cell. The volume of the structural spheres is: $V_{s\sigma}=\pi/6D^3(1+3N)$. Having account of the particle ratios, the structural voluminosity is written as: $\upsilon_\sigma = \chi_v\chi_a\chi_\sigma\upsilon_\phi$, where $\chi_\sigma=(1+N)^3/(1+3N)$ is the flocculation factor. The coarse particles embedded in the mass of finer particles may also be included into the packing by the equation of mixed fractions: $e=e_fC$, or, in terms of the saturated water content, $w = e_fC/G$; where C is the clay fraction and G, the specific gravity of solids. As the Atterberg limits are particular cases of the saturated water content, the plasticity index can be expressed as: $Ip = AC$, where $A = (\upsilon_L-\upsilon_P)/G$ is the Skempton's colloidal activity of clays.

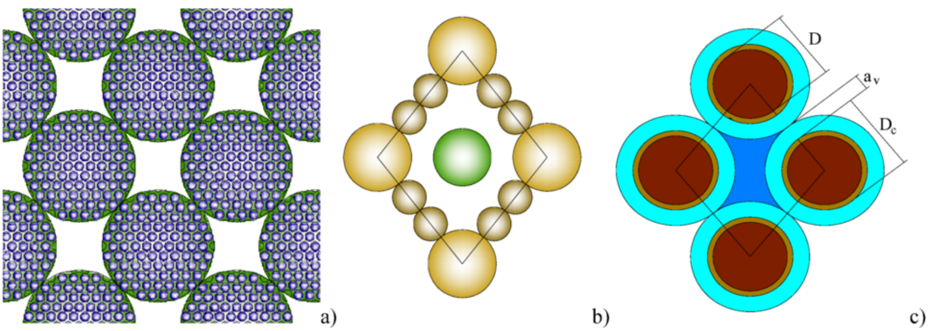

Figure 4. Rhombic packing: a) Idealized fabric of Yong and Sheeran [2], b) Idealized fabric of Collins and McGown [3], and c) Double layer, diameter of contact, and equivalent diameter.

Due to the difficulty of defining the equivalent diameter, D, for fine soils, there is a deviation of the structural voluminosity from the real voluminosity: $d = \upsilon_\sigma - \upsilon$. So that, the void ratio, the saturated water content, and the plasticity index are written in terms of two parameters, χ_1 and $\upsilon_{\phi P}$, that stand for all the individual features:

$$e = \chi_1(\upsilon_\phi - \upsilon_{\phi P}) \qquad w = \frac{\chi_1}{G}(\upsilon_\phi - \upsilon_{\phi P}) \qquad I_p = \frac{\chi_1}{G}(\upsilon_{\phi L} - \upsilon_{\phi P}) \qquad (3)$$

5. Shear strength of clays at critical state

In modern soil mechanics, it is clear that overconsolidated clays and dense sands are dilatant, and normally consolidated clays and loose sands are contractive [11]. This means that the consolidated drained angle of friction, $\varphi_{CD,}$ of normally consolidated clays does not depend on the initial void ratio; except for the critical state, for which $e_{dilatant} = e_{contractive}$. For the rhombohedron, Eq. (3) can be unfolded as follows:

$$w_{cs} = \frac{6\chi_1}{\pi G}\left(\cos^2\varphi_{cs}\sqrt{3-2\cos^2\varphi_{cs}} - \chi_2\right) \qquad (4)$$

In this equation, the water content, w_{cs}, can be appropriately substituted by the liquid limit, w_L, the plasticity index, I_P, or the clay fraction, C.

6. Shear strength of clay formations

It is a known fact that points representing the same clay geological formation tend to group along a straight line in the Casagrande's plasticity chart. This is mainly due to the fact that the clay fraction that composes the layer is the same; and, the constants χ_1 and χ_2 become characteristics of such formation. But clay soils have the property to change structure according to the requirements of the environment. Due to an increase in the clay fraction, coarse particles forming a structural assembly with clay filler become embedded grains. The order of flocculation may increase to accommodate a larger amount of water in a cluster of fine particles. Flocculated structures of clay can change from flocculent to dispersed structures [11]. In these cases, constants χ_1 and χ_2 change to a new value, so that the angle of critical friction associated to the change.

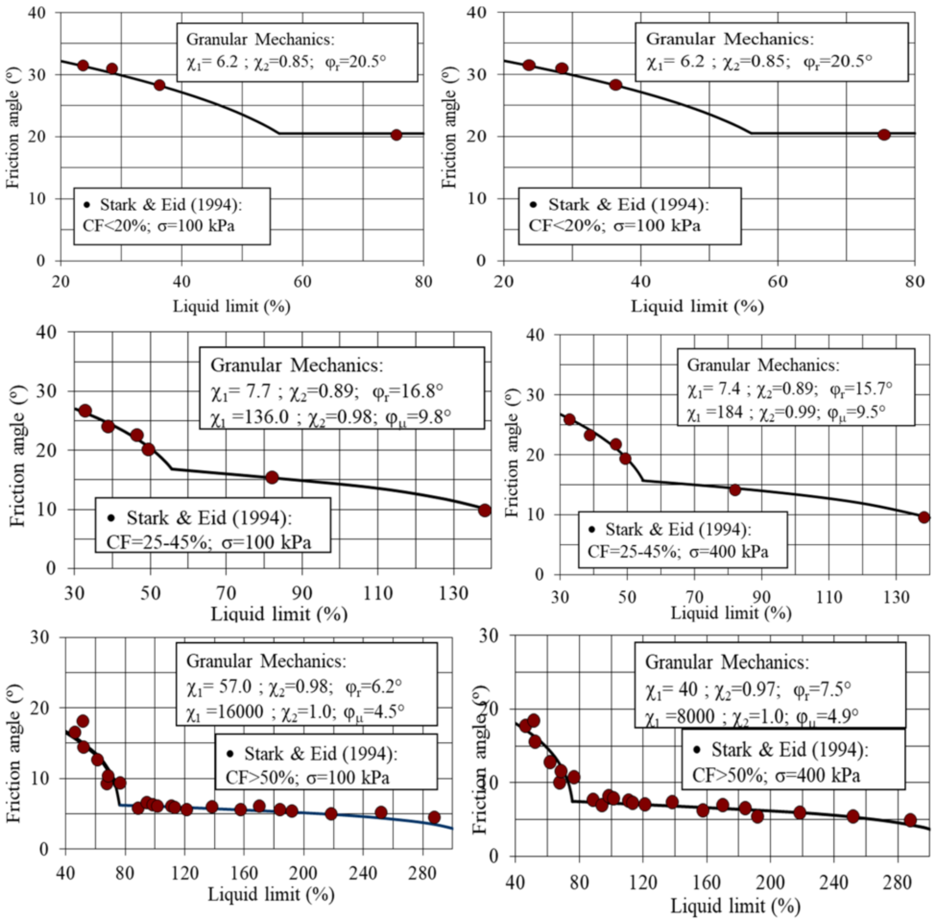

Figure 5. The consolidated drained friction angle as a function of the liquid limit.

The strength of clay geological formations has been better studied in artificial mixtures of coarse soil and clay. For example, the experiments of Stark and Eid [12], which relate the liquid limit to the friction angle of the critical state in soil mixtures, reveal that the change in structure is more evident as the clay fraction is increased. For mixtures with low clay content, the final friction angle depends on the coarse fraction and, therefore, is high and constant, on the order of 20° (Figure 5). These results also agree with the qualitative observations of Lambe and Whitman [13]. Mixtures with a higher clay content exhibit a second curved section, described by Eq. (4), but with a higher value of χ_1. It is important to note that, for $\chi_1 = \infty$, Eq. (4) is transformed into the equation of a horizontal line, which represents a purely granular material or a clay in a totally dispersed state. In the Stark and Eid tests, the first angle of critical friction is 16°, and the second, 9.7°. In mixtures with a high clay content, the first section does not exist due to the definition of the liquid limit, and the second section starts with $\varphi_{\mu1}$=17°, and ends with $\varphi_{\mu2}$=7.0°. However, even this angle of friction varies until reaching the value $\varphi_{\mu2}$=4.5°, corresponding to the total dispersed state.

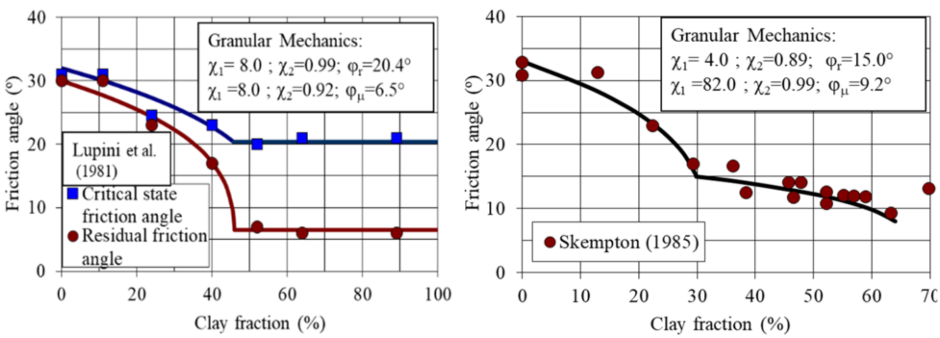

Figure 6. The consolidated drained friction angle as a function of the clay fraction.

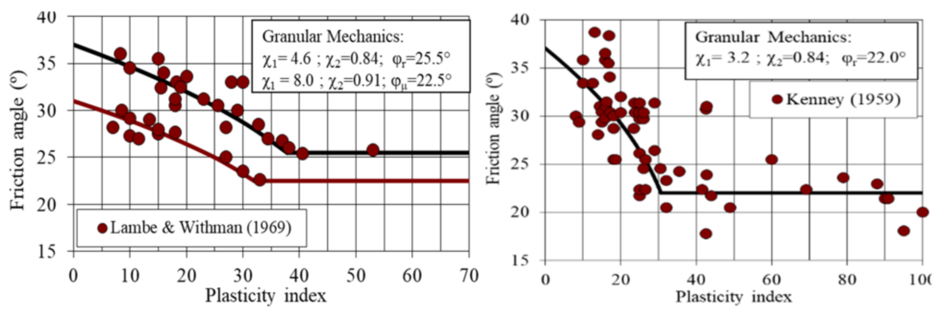

Figure 7. The consolidated drained friction angle as a function of the plasticity index.

These results are corroborated by the tests reported by numerous authors. For instance, the tests carried out by Lupini et al. [14] show that the behavior of the mixture changes from a clay fraction of 46%, becoming constant the CD friction angle. This means that the coarse material ceases to have a structural participation in the mixture from C = 46%. On the other hand, it should be advertised that, actually, the friction angles correspond to a lightly overconsolidated clay, one for the peak condition and other for the critical state. In the Skempton tests [15], the change of the clay behavior occurs when the clay fraction is 30%, but the friction angle in the second section varies according to Eq. (4), until reaching the residual value of 9.2° (Figure 6b). The tests on two marine clays, reported by Lambe and Whitman [13] (Figure 7a), show a behavior similar to those of Lupini et al. In this context, the data collected by Kenney [16] has a very high dispersion, as long as the fraction or the composition of the clays has not been considered. But it is illustrative to mention that, for this case, a good fit is obtained by making χ_1=3.2 and χ_2=0.84 (Figure7b).

7. Conclusions

All the characteristics of particulate materials may be studied in a simple and direct way using the packings of spheres. The mapping of the packing two-valued curve into the compression two-valued curve associates the dilatant packing to an overconsolidated clay, and the contractive packing to a normally consolidated clay. So that, there is a unique value for the consolidated-drained friction angle of normally consolidated clays. However, due to the duality of packings, a clay geological formation may be characterize by means of the law for overconsolidated clays just for the critical state. Indeed, the consolidated-drained friction angle for normally consolidated is related to the coefficient of lateral pressure at rest, the liquid limit, the plasticity index, and the clay fraction. All of these curves fit very well with the experimental data reported by several authors.

References

[1] M. Budhu, *Soil Mechanics and Foundations*, John Wiley & Sons, New Jersey, 2011.
[2] R.N. Yong & D.E. Sheeran, Fabric unit interaction and soil behavior, *Proc. International Symposium on Soil Structure, Gothenburg, Sweden*, (1973) 176–183.
[3] K. Collins & A. Mcgown, The form and function of microfabric features in a variety of natural soils, *Geotechnique*, vol. 24 (2), 223-254.
[4] A. Casagrande (1936), Characteristics of cohesionless soils affecting the stability of slopes and earth fills, *Contributions to Soil Mechanics*, BSCE, (1974), 257-276.
[5] D.H. Trollope, *The Stability of wedges of granular materials*, Ph.D. Thesis, University of Melbourne, 1956.
[6] S.F. Edwards, The equation of stress in a granular material, *Physica* A (1998), 249, 226.
[7] C. Yanqui, *Statics of Gravitating Discontinua*. M. Sc. Thesis, University of South Carolina, 1982.
[8] E.W. Brooker & H.O. Ireland, Earth pressures at rest related to stress history, *Canadian Geotechnical Journal*, Vol. 11 (1), (1965).
[9] R.D. Holtz & W.D. Kovacs. *An Introduction to Geotechnical Engineering*, Prentice Hall, New Jersey.1981.
[10] P.W. Rowe, The stress-dilatancy relation for static equilibrium of an assembly of particles in contact, *Proceedings Royal Society of London*, Ser. A, Vol. 269, (1962), 500-527.
[11] J.K. Mitchell, *Fundamentals of Soil Behavior*, John Wiley & Sons, New York, 1993.
[12] T.D. Stark & H.T. Eid, Drained residual strength of cohesive soils, *Journal of geotechnical engineering*, ASCE, vol. 120 (5), (1994), 856-871.
[13] T.W. Lambe & R.V. Whitman, *Soil Mechanics*, John Wiley & Sons, New Jersey, 1969.
[14] J.F. Lupini, A.E. Skinner & P.R. Vaughan, The drained residual strength of cohesive soils, *Geotechnique*, Vol. 31 (2), (1981), 181-213.
[15] A.W. Skempton, Residual strength of clays in landslides, folded strata, and the laboratory, *Geotechnique*, vol.35 (1), (1985), 3-18.
[16] T.C. Kenney, Discussion. *J. Soil Mechanics. and Foundations*, ASCE, Vol. 85 (3), (1959), 67-69.